Results in Physics 10 (2018) 504–511

Contents lists available at ScienceDirect

Results in Physics

journal homepage: www.elsevier.com/locate/rinp

Inhibition performance of three naphthyridine derivatives for mild steel corrosion in 1M HCl: Computation and experimental analyses

Chandrabhan Verma[a,b], Ahmad A. Sorour[c], Eno.E. Ebenso[a,b,*], M.A. Quraishi[c,d,*]

[a] Department of Chemistry, School of Mathematical & Physical Sciences, Faculty of Agriculture, Science and Technology, North-West University (Mafikeng Campus), Private Bag X2046, Mmabatho 2735, South Africa
[b] Material Science Innovation & Modelling (MaSIM) Research Focus Area, Faculty of Agriculture, Science and Technology, North-West University (Mafikeng Campus), Private Bag X2046, Mmabatho 2735, South Africa
[c] Center of Research Excellence in Corrosion, Research Institute, King Fahd University of Petroleum & Minerals, Dhahran 31261, Saudi Arabia
[d] Department of Chemistry, Indian Institute of Technology (Banaras Hindu University), Varanasi 221005, India

ARTICLE INFO

Keywords:
Mild steel
Naphthyridines
Aggressive solution
Electrochemical studies
AFM
Acid inhibitors

ABSTRACT

The influence of three naphthyridines (NTDs) on acidic dissolution of mild steel was evaluated using experimental methods. Protection abilities of the NTDs molecules are increases with their concentrations. Maximum inhibition efficiency of 98.69% was observed for NTD-3 molecule at its 4.11×10^{-5} mol/L^{-1} concentration. The inhibition efficiencies of NTDs molecules followed the order: NTD-1 (96.1%) < NTD-2 (97.4%) < NTD-3 (98.7%). Polarization study showed that NTDs acted as mixed type inhibitors and they preferably block the active sites accountable for the corrosion. EIS study suggested that the NTDs inhibit corrosion because of their adsorption at electrolyte/metal interfaces and their adsorption followed Langmuir adsorption isotherm. AFM analysis was adopted to support the adsorption inhibitive behavior of NTDs.

Introduction

Heteroatoms containing organic compounds represent an important category of inhibitors for metallic corrosion which can be used during pickling of metals and alloys and acidization of oil well [1-5]. Previous studies have shown that heterocyclic compounds act as effective inhibitors for metallic corrosion. Their effectiveness is based on the presence of heteroatoms, π-electrons, non-bonding electrons and aromatic rings [6]. The adsorption of these inhibitors be contingent upon more than a few factors including nature of substituents, adsorption sites, metal, testing medium and solution temperature etc. [7]. Generally, adsorption of organic compounds results into the formation of protective and inhibitive film that retards the metallic dissolution through avoiding the direct contact of metals and aggressive media. Recently, naphthyridine derivatives have attracted extensive devotion due to their impending natural happenings such as antibacterial, anti-inflammatory, anti-hypertensive, anti-platelet, anti-arrhythmics, herbicide safeners, immunostimulants activities [8–10].

Generally, naphthyridines derivatives are associated with high degree of functionality and solubility in polar media like 1M HCl solution that make them suitable anticorrosive candidates. Kalaiselvi et al. [11] studied the performance of three 1, 8-naphthyridine derivatives using electrochemical, chemical and solution analysis (AAS) techniques. The experiments were performed on mild steel in acid solution. Results of the study showed that 1, 8-naphthyridine derivatives acted as good inhibitors and they showed as much as 99.21% of efficiency at as low as 0.3×10^{-3} mol/L concentration. In another study, Álvarez-Manzo et al. [12] synthesis and tested the inhibition efficiency of five 1, 8-naphthyridines derivatives. They observed the maximum protection ability of around 99% at 500 ppm (2.06 mol/L) concentration. The influence of three 1, 8-naphthyridines derivatives on mild steel has also been investigated by Ansari and Quraishi [13]. The maximum inhibition efficiency of best inhibitor was about 93% at 200 ppm (0.69×10^{-3} mol/L) concentration.

Herein, three 1, 6-naphthyridine derivatives (NTDs) have been produced from the earlier reported method and investigated their corrosion inhibition efficiency on mild steel in 1M HCl. The criteria for selection of the naphthyridines is grounded on the fact that they contain five nitrogen atoms (heteroatoms with lone pair of electrons) in addition to hydroxyl groups (high degree of functionality), aromatic ring

* Corresponding authors at: Department of Chemistry, School of Mathematical & Physical Sciences, Faculty of Agriculture, Science and Technology, North-West University (Mafikeng Campus), Private Bag X2046, Mmabatho 2735, South Africa (E.E. Ebenso). Center of Research Excellence in Corrosion, Research Institute, King Fahd University of Petroleum & Minerals, Dhahran 31261, Saudi Arabia (M.A. Quraishi).
E-mail addresses: Eno.Ebenso@nwu.ac.za (E.E. Ebenso), maquraishi.apc@itbhu.ac.in (M.A. Quraishi).

https://doi.org/10.1016/j.rinp.2018.06.054
Received 4 June 2018; Received in revised form 22 June 2018; Accepted 24 June 2018
Available online 28 June 2018

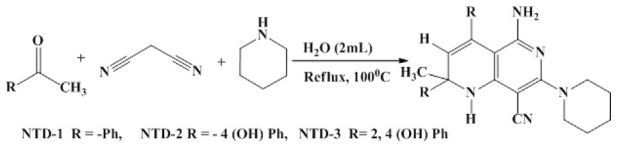

Fig. 1. Synthetic rout of studied NTDs.

(high π-electrons density), and non-bonding electrons through which these compounds are likely to adsorb on mild steel surface efficiently [14–21].

Experimental methods

Metallic sheet purchased from market with elemental composition reported in our earlier publications was used for experimental works as per the earlier reported methods [23,24]. Electrolyte was 1M HCl which was also prepared as described in our previous reports. The investigated naphthyridine derivatives (NTDs) were synthesized affording to the beforehand designated method [22]. The synthetic scheme is revealed in Fig. 1 and informations correlated to the NTDs molecules are given in Table S1. The methodologies and experimental procedures for weight loss, surface (AFM), and electrochemical studies were same as we reported in our previous reports [23,24]. The DFT study was carried out as described in our previous reports [23,24].

Supplementary data associated with this article can be found, in the online version, at https://doi.org/10.1016/j.rinp.2018.06.054.

Results and discussion

Electrochemical study

Open circuit potential (OCP)

The OCP versus time curves with and without NTDs are given in Fig. 2. OCP is the potential that has established on the mild steel working electrode deprived of smearing any outside current. On observing Fig. 2 carefully it can be seen that inhibited (by NTDs) OCP versus time curves have been moved towards more negative course derived of varying the collective features of the curves. Generally, this type of potential shifts are related to the disintegration or dissolution of surface metal oxides layers (Fe_3O_4 and Fe_2O_3) and adsorption of the inhibitor (NTD) molecules at the interfaces [25,26]. It is important to

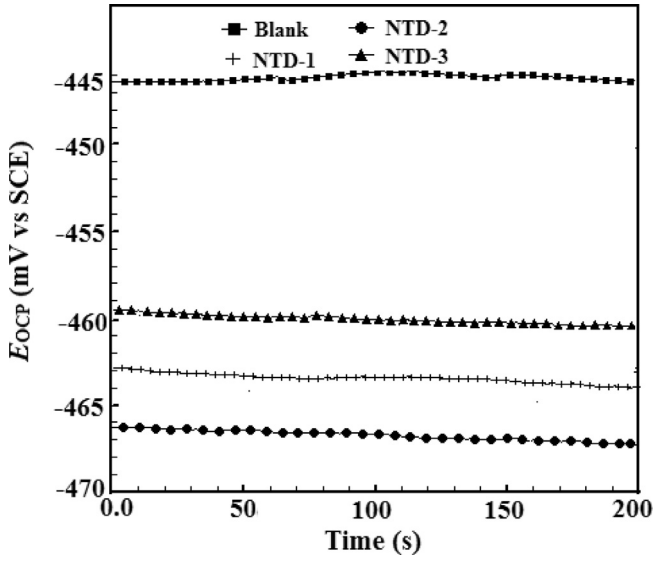

Fig. 2. OCP vs time curves for mild steel dissolution in 1M HCl in absence and presence of optimum concentration of NTDs.

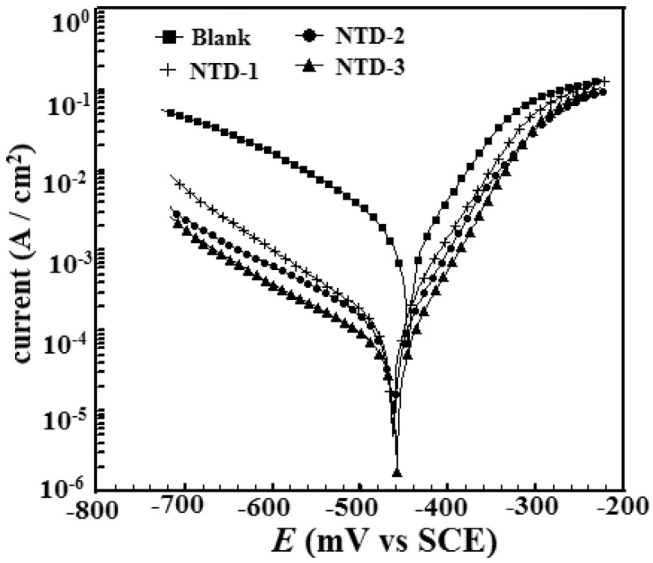

Fig. 3. Polarization curves for mild in absence and presence of optimum concentration of NTDs.

mention that whenever a metal surface exposed to acidic aggressive solution then rapid dissolution of its oxides takes place that results into the variation in the OCP. A straight OCP versus time curves are the indication for establishment of steady state potential (E_{corr}). Generally, organic inhibitors like NTD molecules inhibit both anodic and cathodic reactions however in present cases inhibited OCP versus time curves shifted in negative (cathode) direction which suggests that NTDs have major influence on cathodic (hydrogen evolution) reaction [27]. The values of E_{corr} of studied compounds followed the order: NTD-3 > NTD-1 > NTD-2, instead of expect NTD-1 > NTD-2 > NTD-3 order of E_{corr}. This finding suggests that NTD-2 showed relatively more anodic behavior that NTD-1 and NTD-3. The tested compounds followed the anodic dominance order: NTD-3 > NTD-1 > NTD-2. Similar explanations have been stated in numerous other reports [28–30]. Fig. 2 represents the linear lines suggesting that oxide layer have been removed completely from the surface and adsorption of the NTDs molecules occurred after 200 s immersion time.

Polarization

The Tafel polarization curves for the dissolution of mild steel in 1M HCl are revealed in Fig. 3. These Tafel curves have been extrapolated to get some common polarization indices like i_{corr} (corrosion current density), E_{corr} (corrosion potential), β_c (cathodic Tafel slope) and β_a (anodic Tafel slope). These polarization indices along with the percentage of inhibition efficiency (η%) are presented in Table 1. Review of the Table revealed that shapes of protected and non-protected polarization curves are very much similar which implies that NTDs molecules retards corrosive disintegration of mild steel by imposing inhibitive film and blocking the active sites deprived of altering the mechanism of disintegration. More so, presence of NTDs in the corrosive medium did not cause any substantial change in value of E_{corr}

Table 1
Tafel polarization parameters for mild steel in 1M HCl solution in absence and at optimum concentration of NTDs.

Inhibitor	E_{corr} (mV/SCE)	i_{corr} (μA/cm^2)	β_a (mV/dec)	$-\beta_c$ (mV/dec)	θ	η%
Blank	−445	1150	70.5	114.6	–	–
NTD-1	−463	84.2	60.3	186.1	0.927	92.7
NTD-2	−467	61.3	60.4	154.6	0.947	94.7
NTD-3	−459	36.4	58.2	178.2	0.969	96.9

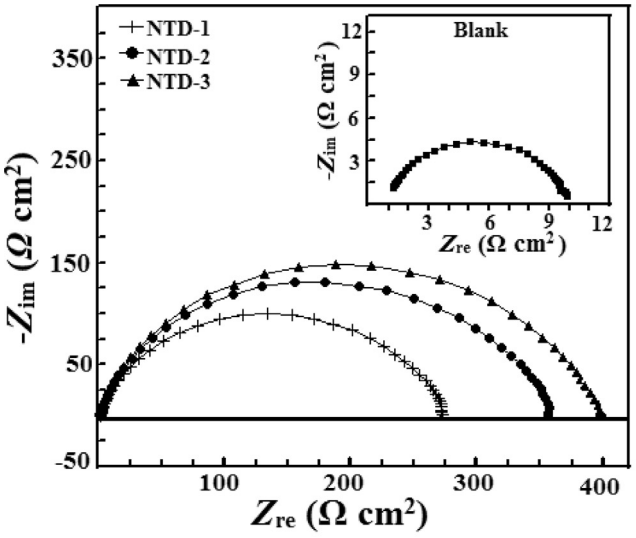

(a)

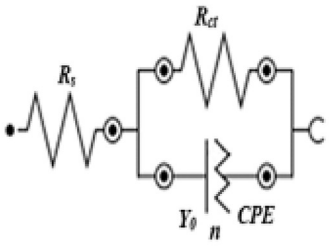

(b)

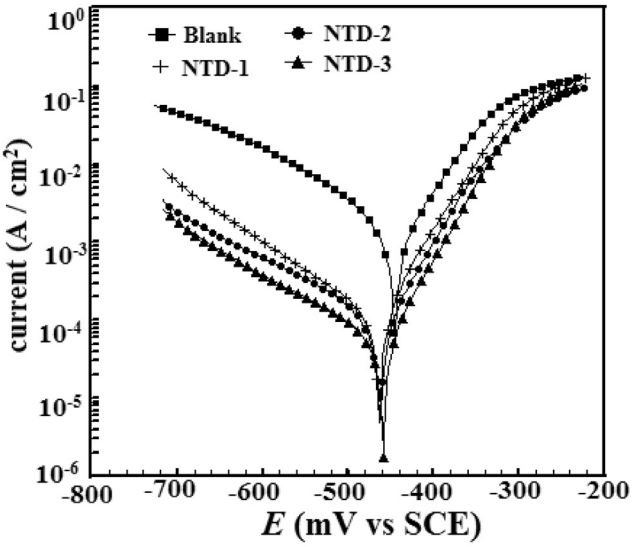

(c)

Fig. 4. a-c: (a): Nyquist plot for mild steel in 1M HCl without and with optimum concentrations of NTDs. (b): Equivalent circuit model used to fit the EIS data. (c): Bode (log f vs log $|Z|$) and phase angle (log f vs α^0) plots for mild steel in 1M HCl in absence and presence of optimum concentration of NTDs.

which implies that NTDs act as mixed type inhibitors [31]. However, compared to the β_a, the values of β_c showed somewhat more variation which suggested that NTDs acted as principally cathodic type inhibitors [32].

Table 2
EIS parameters obtained for mild steel in 1M HCl in without and with optimum concentration of NTDs.

Inhibitor	R_s (Ω cm^2)	R_{ct} (Ω cm^2)	C_{dl} (μF cm^{-2})	n	θ	η%
Blank	1.12	9.58	106.21	0.827	–	–
NTD-1	1.05	264.7	42.82	0.854	0.964	96.4
NTD-2	1.00	344.9	41.81	0.856	0.972	97.2
NTD-3	1.11	386.1	33.09	0.859	0.975	97.5

Electrochemical impedance spectroscopic measurements

Nyquist plots with and without NTDs are presented in Fig. 4a which revealed a single semicircle under both situations. Formation of the single semicircle is generally resulted due to the involvement of single charge transfer mechanism [33,34]. The diameter of the semicircle generally increases with increasing the resistance for the charge transfer phenomenon. Increased diameter of the Nyquist plots for inhibited (by NTDs) as compared to uninhibited one is resulted due to formation of protective surface film by NTDs [35]. It is important to mention that NTDs have several adsorption centers through which it can easily adsorb at interfaces and impose barrier for charge transfer from metal to electrolyte. Equivalent circuit depicted in Fig. 4b was employed to calculate EIS parameters. The evaluated EIS indices along with percentage of inhibition efficiency are shown in Table 2. Implementation of the CPE as an alternative of pure capacitor for acid catalyzed electrochemical corrosion of mild steel (or other metals and alloys) provides superior approximation. Impedance of the CPE that is constant phase element used in the equivalent circuit can be accessible as follows [36]:

$$Z_{\mathrm{CPE}} = Y_0 (j\omega)^{-n} \tag{4}$$

where the Y_0 is a proportionality factor and n is the *CPE* exponent (phase shift). j is the imagined number and ω is the angular frequency. Generally, the value of n lies in between 0 and 1 and being used as a gauss for surface homogeneity measurement. The adsorption of inhibitors on metal/electrolyte (acid solution) interface results in the formation of a differential capacitance rather than an ideal capacitance. It is obvious that adsorption of inhibitors (NTDs) at the interface results in the formation of double layer whose capacitance (C_{dl}) can be obtained as follows [37]:

$$C_{dl} = \frac{Y_0 \omega^{-n}}{\sin(n(\pi/2))} \tag{5}$$

The inspection of the data revealed that R_{ct} values augmented in the presence of NTDs which can be credited because of the establishment of defensive covering by NTDs on the mild steel surface [31,5]. More so, the C_{dl} values are higher for uninhibited solution than that for inhibited solution. The decreased values of C_{dl} value in presence of NTDs (or other inhibitors) are generally resulted because of the amplified breadth of the electric double layer generated at the electrolyte/ metallic interfaces through their (NTDs) adsorption [5].

The Bode plots for the mild steel dissolution in 1M HCl in absence and presence of optimum concentrations of NTDs are shown in Fig. 4c. In the Bode plots, the value of left legend (/Z/) represents the impedance of the Bode plots while right legend (α°) value represents the phase angle. Generally, phase angle value is related with the surface morphology and its inferior value proposes the higher surface irregularity or inhomogeneity and vice versa. Development of the single maxima (one time constants) in Bode plots supported the conclusion derived from Nyquist plots that the metallic dissolution with and without NTDs involves the single charge transfer mechanism [38,39]. Careful evaluation of the Bode plots reveals that the magnitude of phase angles for three studied inhibitors have significantly enhanced and thereby surface smoothnesses have been amplified because of the adsorption of the inhibitors on the metallic surface as compared to

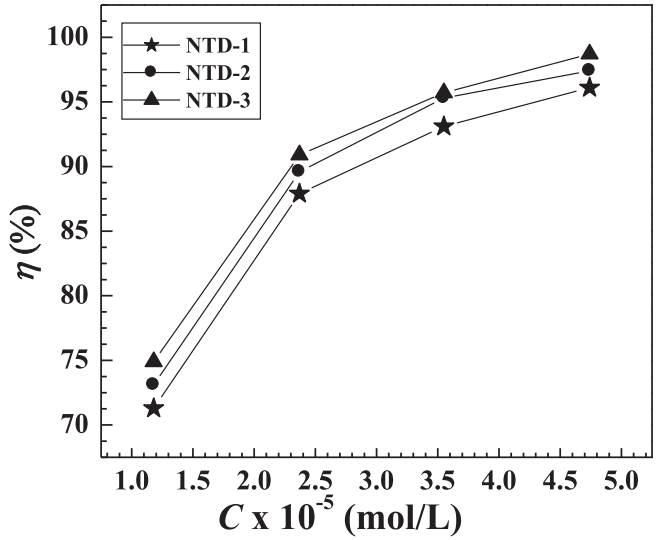

Fig. 5. Variation of inhibition efficiency with NTDs concentration.

uninhibited specimen [40].

Weight loss measurements

Effect of NTDs concentration

The variation in the η%, corrosion rate (C_R) and surface coverage with NTDs concentration is shown in Fig. 5 and Table 3. From the results it is clear that the inhibition efficiency increases as the concentration of NTDs increases. Results showed that the NTD-3 showed the maximum η% of 98.69% followed by NTD-2 (97.38%) and finally by NTD-1 (96.08%) at as low as 4.11×10^{-5} mol/L concentration. Weight loss experiments were also carried out after keeping the NTDs concentrations more than 4.11×10^{-5} mol/L however no appreciable increase in the inhibition performance of NTDs were observed which suggested that 4.11×10^{-5} mol/L is optimum concentration. The optimum concentration was employed for electrochemical studies. The higher inhibition efficiency of the investigated 1, 6-naphthyridines derivatives synthesized in our lab as compared to previously reported 1, 8-naphthyridines derivatives is due some structural difference between them. Higher molecular weight, presence of polar functional groups (−OH, −CN, $-NH_2$), π-electrons, non-bonding electrons and aromatic rings favor the adsorption of investigated 1, 6-naphthyridines derivatives as compare to 1, 8-naphthyridines derivatives.

Table 3
The weight loss parameters obtained for mild steel in 1M HCl containing different concentrations of NTDs.

Inhibitor	Conc (mol/L)	C_R (mg cm^{-2}h^{-1})	Surface coverage (θ)	η%
Blank	0.0	7.66	–	–
NTD-1	1.18×10^{-5}	2.2	0.713	71.3
	2.37×10^{-5}	0.93	0.879	87.9
	3.55×10^{-5}	0.53	0.931	93.1
	4.74×10^{-5}	0.30	0.961	96.1
NTD-2	1.18×10^{-5}	2.06	0.731	73.1
	2.37×10^{-5}	0.80	0.896	89.6
	3.55×10^{-5}	0.36	0.953	95.3
	4.74×10^{-5}	0.20	0.974	97.4
NTD-3	1.18×10^{-5}	1.93	0.749	74.9
	2.37×10^{-5}	0.70	0.909	90.9
	3.55×10^{-5}	0.33	0.957	95.7
	4.74×10^{-5}	0.10	0.987	98.7

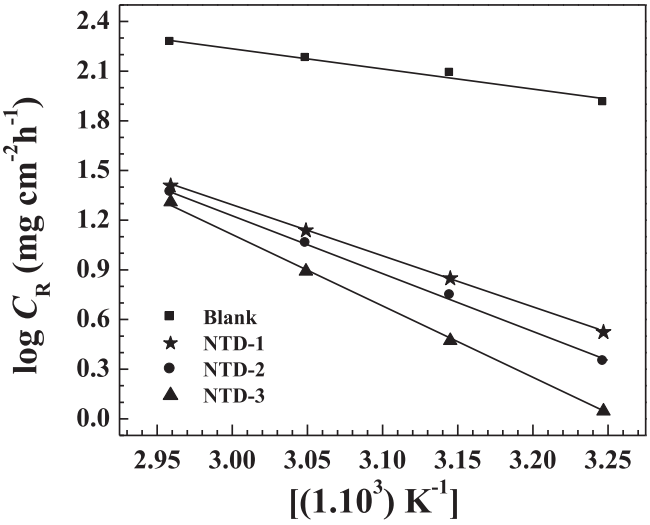

Fig. 6. Arrhenius plots for the corrosion rate of mild steel versus the temperature in 1M HCl.

Effect of temperature

The C_R and η% values derived at different temperature (308–338 K) with (optimum concentration) and without NTDs are given in Table S2. The inspection of the results revealed that C_R values rises and the η% decreases on growing solution temperature for both inhibited and uninhibited solutions. This temperature dependency of C_R was estimated using Arrhenius equation [41]:

$$C_R = A \exp\left(\frac{-E_a}{RT}\right) \tag{7}$$

In above equation all symbols have their usual meaning. The value of apparent activation energy (E_a; kJ mol^{-1}) for inhibited and uninhibited solutions was derived from Arrhenius plots of log C_R versus $1/T$ (Fig. 6). The values of E_a increased from 28.48 kJ mol^{-1} (blank) to 54.18 kJ mol^{-1}, 67.44 kJ mol^{-1}, and 83.88 kJ mol^{-1} in presence of NTD-1, NTD-2 and NTD-3, respectively. The increased value of E_a in presence of NTDs molecules indicates that corrosion progression has becomes hard due to establishment of the energy barrier in presence of these inhibitors. Order of the η% can also be validated by the values of E_a (kJ mol^{-1}) for these tested inhibitor molecules [42,43]. The highest value of E_a (kJ mol^{-1}) for NTD-3 among the tested compounds shows that NTD-3 is the most effective inhibitor, while the lowest value of E_a (kJ mol^{-1}) for NTD-1 indicates that NTD-1 is the least effective corrosion inhibitor.

Adsorption isotherms

In the present case, adsorption behavior of NTDs molecules was tested using some commonly used isotherms namely, Temkin, Frumkin and Langmuir but Langmuir isotherm gave the best fit. Following equation represents the simplest form of Langmuir equation [44]:

$$K_{ads} C = \frac{\theta}{1-\theta} \tag{8}$$

The symbols used in the Langmuir equations have their usual meaning. The Langmuir isotherm represented in Fig. 7 which is designed among log ($\theta/1-\theta$) vs log $C_{(mol/L)}$. The K_{ads} is connected to the standard free energy (ΔG^0_{ads}) of adsorption progression by the relation [45]:

$$\Delta G^0_{ads} = -RT \ln(55.5 K_{ads}) \tag{9}$$

Here, the 55.5 represents the aqueous concentration in 1M HCl acid solution and other digits have their usual meaning. The calculated values of K_{ads} and ΔG^0_{ads} are given in Table S2. From the results it can be seen that values of K_{ads} follow the order: NTD-3 > NTD-2 > NTD-1

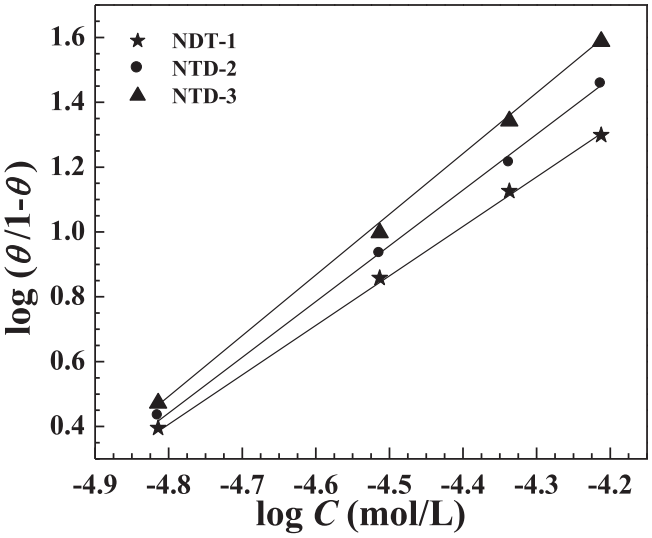

Fig. 7. Langmuir isotherm plots for the adsorption of NTDs on mild steel surface in 1M HCl.

and thereby values of surface coverage also follows the same trend (according to equation (8)). The observed values of K_{ads} and surface coverage well justify the order of the η% of the tested compounds obtained by weight loss and electrochemical measurements. The ΔG^0_{ads} values fluctuates in between -34.84 and $-38.78\,kJ\,mol^{-1}$, which signify that NTDs adsorb by physiochemisorption mode [46,47]. From equation (9) it is clear that greater the value of K_{ads}, lower will be value of ΔG^0_{ads} (more negative) and greater will be spontaneity of the inhibitors adsorption. Therefore, a more negative value ΔG^0_{ads} is consisted with high surface coverage. From the results shown in Table S2 it is concluded that the surface coverage values of these inhibitors follows the order: NTD-3 > NTD-2 > NTD-1.

Atomic force microscope (AFM) analysis

The AFM images of the working electrode surfaces are shown in Fig. 8. The uninhibited mild steel surface is highly corroded and damaged and it has the average surface roughness of 392 nm. It is significant to remark that in the absence of NTDs, aggressive attacks of the acidic medium resulted in to the damaging of the surface morphology. However, in presence of NTDs (Fig. 8b-d) the surface smoothness significantly upgraded owing to the establishment of defensive film by NTDs on mild steel surface. The calculated surface roughness were 143, 86, and 63 nm in presence of NTD-1, NTD-2 and NTD-3, respectively.

DFT study

The frontier molecular orbital pictures of NTD-1, NTD-2 and NTD-3 are presented in Figs. 9 and 10 and several computational indices are given in Table 4. It is important to mention that inputs of the DFT study can be correlates with the order of the chemical reactivity or the adsorption tendency of NTD-1, NTD-2 and NTD-3 molecules over the metallic surface. In general a more reactive compound is associated with higher corrosion protection ability as compared to the chemically less reactive molecule. Obviously, a high value of E_{HOMO} is consistent with high chemical reactivity and vice versa. Results depicted in Table 4 showed that values of E_{HOMO} are increasing (in positive) on moving from NTD-1 to NTD-3 which implies that electron donating abilities s and thereby protection tendencies of these compound are increasing in the similar arrangement [23,24]. Similarly, value of E_{LUMO} is related with electron accepting ability of the inhibitor (NTDs) molecules. Careful observation of the results presented in Table 4 suggested that values of E_{LUMO} are not showing any predicted trend. The

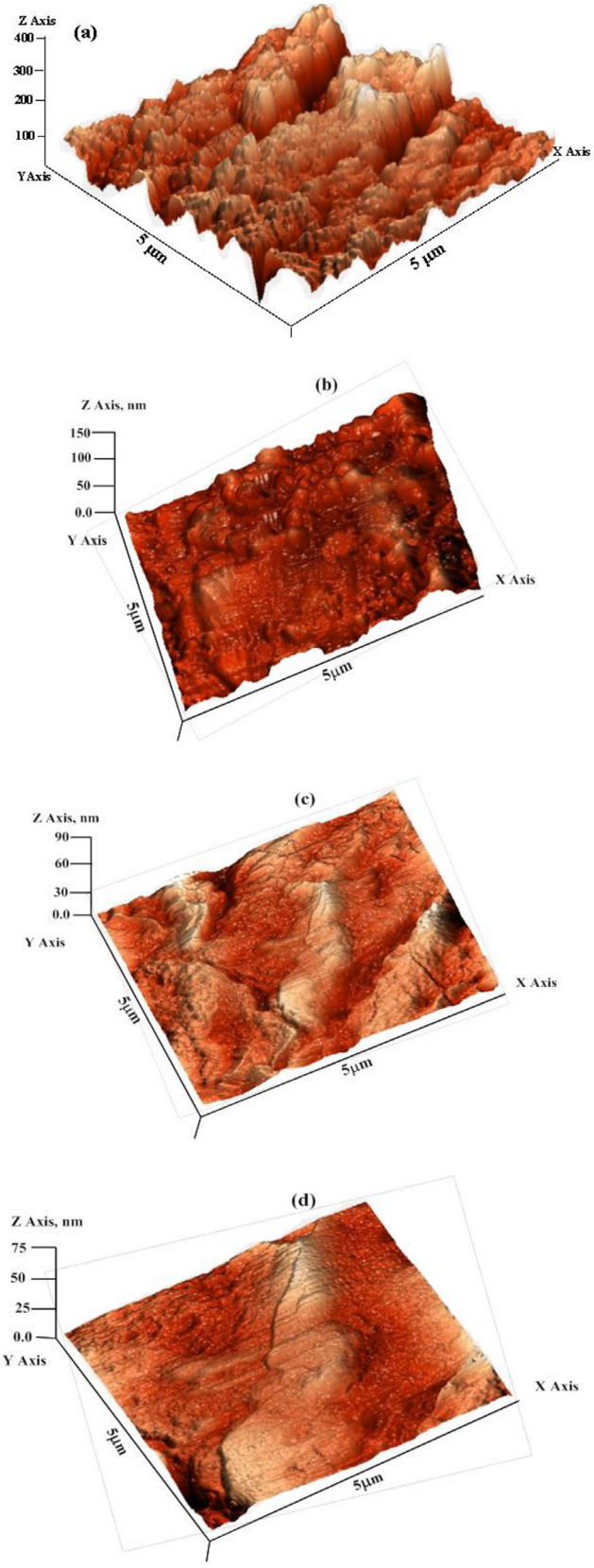

Fig. 8. AFM images of mild steel: (a) in absence of NTDs and in the presence of optimum concentration of (b) NTD-1, (c) NTD-2, and (d) NTD-3.

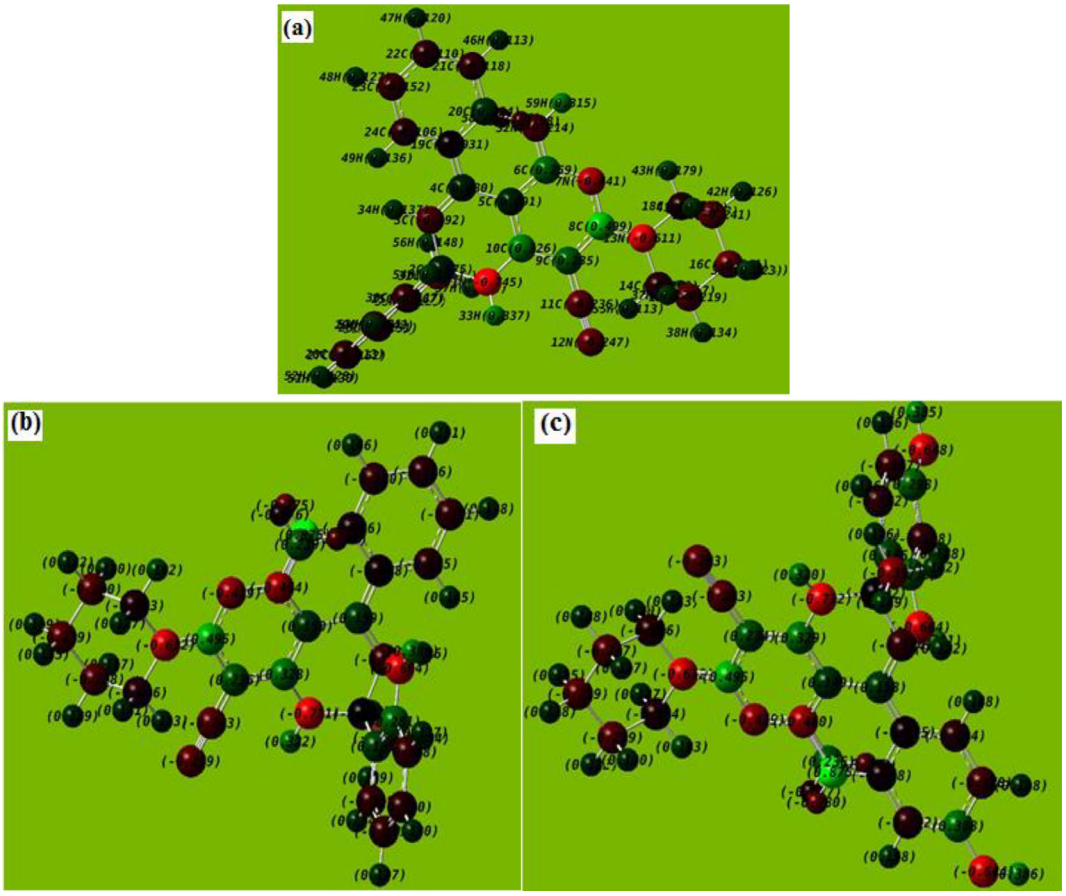

Fig. 9. Optimized frontier molecular orbital structure of (a) NTD-1, (b) NTD-2, and (c) NTD-3.

energy band gap (ΔE) is one of the most significant DFT established reactivity constraint and its inferior values is accompanying with high chemical reactivity. Results showed that values of Δ*E* for NTDs are decreasing in the order: NTD-1 < NTD-2 < NTD-3, which suggests that NTD-3 is most reactive among the tested compounds while NTD-1 is least reactive [23,24]. The most reactive compound is associated with highest inhibition efficiencies and vice versa. On this source, it can be determined that NTDs display the inhibition sequence of: NTD-3 > NTD-2 > NTD-1, which is rendering to the experimental order of their efficacy [23,24]. Softness and hardness are two other relative DFT based indices and both are inversely related to each other. Obviously, a high value of softness or low value of hardness is associated with high chemical reactivity and thereby high protection ability. The softness and hardness values of NTD-1, NTD-2 and NTD-3 presented in Table 4 are according to the predicted trend of inhibition efficiency [23,24]. At last values of dipole moment for NTD-1, NTD-2 and NTD-3 molecules were calculated. It important to mention that when an organic compound approaches and interacts with the metallic surface, it polarize and cover the metallic surface and thereby protects from corrosion. An organic compound having greater value of dipole moment is considered to be more polarizable as compared to the compound having lesser value of dipole moment. In our present study, dipole moment values are increasing on going NTD-1 to NTD-3 which suggests that polarizability thereby protection ability of NTD-1, NTD-2 and NTD-3 molecules are increasing in the same trend.

Mechanism of inhibition

The adsorption of inhibitors (NTDs) at the metal / electrolyte interface takes place by two types of interactions: the physisorption and the chemisorption. Generally, the physical adsorption comprises electrostatic interactions. Chemisorption comprises sharing of charges between inhibitors (NTDs) and metal surface [48,49]. In the present study, the values ΔG^{0}_{ads} varies from -34.84 to -38.78 kJ/ mol which suggest that interaction between metal surface and NTDs involves both physical and chemical interactions [50–53]. Thus it is concluded that initially NTDs are physically adsorbed on metal surface later on chemisorption takes place by charge sharing between metal surface and NTDs molecules. Based on these experimental and theoretical observations a proposed model of NTDs adsorption on mild steel surface in 1M HCl is shown in Fig. 11. The higher η% of investigated NTDs as compared to previously reported naphthyridines derivatives is attributed due to presence of highly basic nature of NTDs. Further, presence of functional moieties (such as −CN, $-NH_2$, −OH), planer structure, and aromatic rings in the NTDs molecules enhance strong bonding between metal and the inhibitors. In our present study, the inhibition efficiency of the investigated NTDs follows the order: NTD-3 > NTD-2 > NTD-1. The difference in inhibition efficiency among the investigated inhibitors can be explained in the terms of relative basicity and the molecular structure of the NTDs. The NTD-2 gives better inhibition performance as corrosion inhibitor than NTD-1 because of the presence of two surplus electron discharging −OH groups. The NTD-3 gives the best performance of 98.7% at 4.11×10^{-5} mol/L concentration as an inhibitor which is attributed to the presence of four surplus electron releasing –OH groups and extensively delocalized π-electrons [54].

Conclusion

From the obtained results following conclusion can be drawn:

1. The corrosion inhibition efficiency of 1, 6-naphthyridines

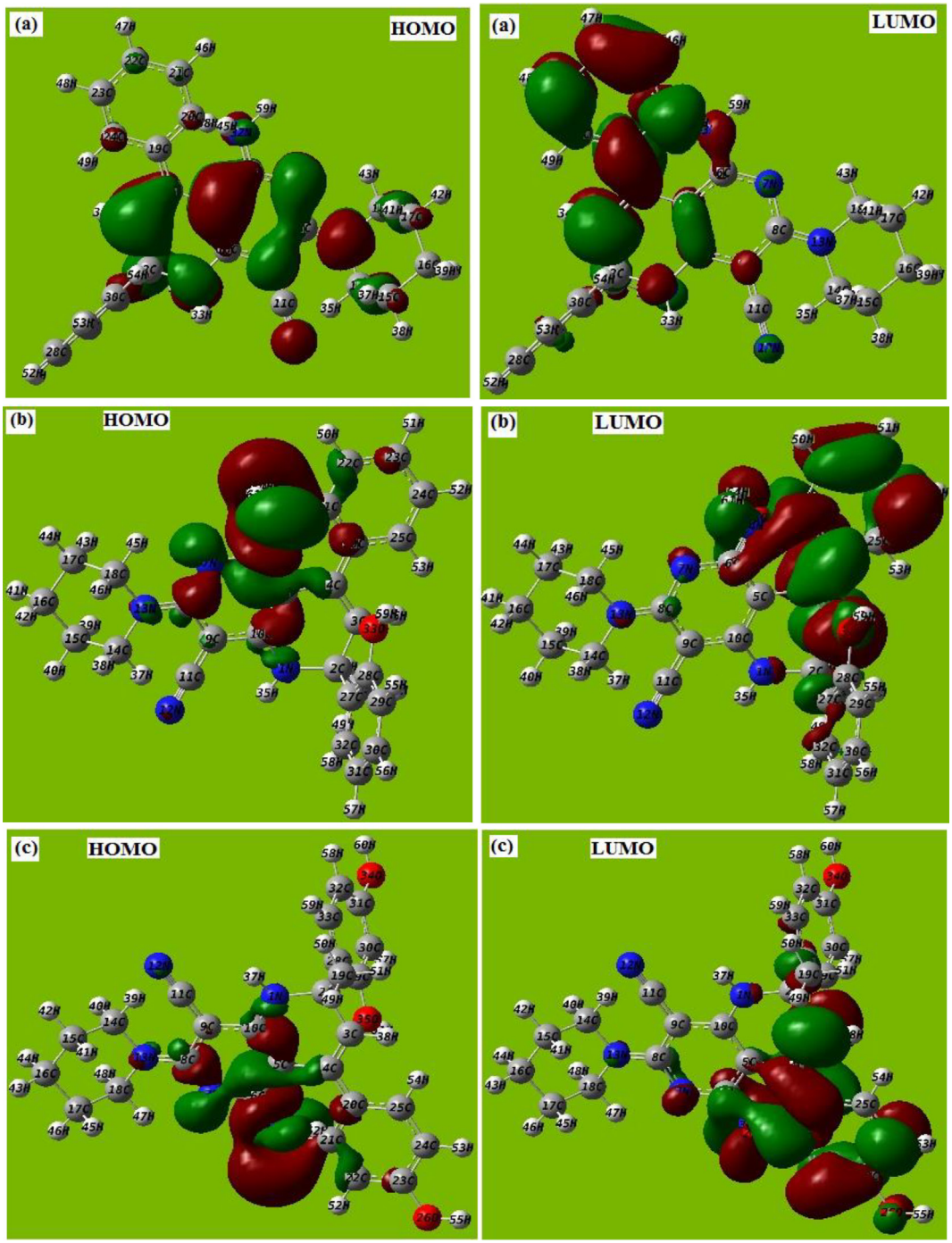

Fig. 10. HOMO and LUMO frontier molecular orbital structure of (a) NTD-1, (b) NTD-2, and (c) NTD-3.

derivatives investigated in the present study are better as compared to 1, 8-naphthyridines derivatives investigated previously by several authors.

2. The η% increases with NTDs concentration. The NTD-3 gave the best inhibition efficiency of 98.7% at 4.11×10^{-5} mol/L concentration.
3. The adsorption of the studied followed the Langmuir adsorption isotherm.
4. Polarization study publicized that the NTDs performed as mixed and predominantly acted as cathodic inhibitors.
5. The AFM results showed that the surface roughness decreases in

Table 4
Quantum chemical parameters for different NTDs.

Inhibitor	Dipole movement (μ)	E_{HOMO} (Hartree)	E_{LUMO} (Hartree)	ΔE (Hartree)	Hardness (ρ)	Softness (σ)
NTD-1	2.8601	−0.17615	−0.04193	0.13422	0.06711	14.900
NTD-2	5.9818	−0.08304	−0.04664	0.0364	0.01820	54.945
NTD-3	7.0490	−0.06972	−0.04246	0.02726	0.01363	73.367

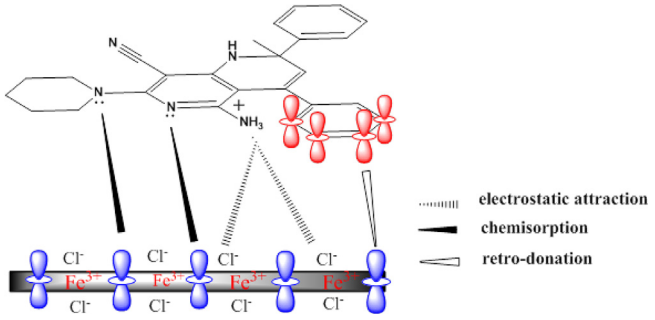

Fig. 11. Pictorial representation of the adsorption behaviour of the NTDs on mild steel in 1M HCl solution.

presence of NTDs, due to establishment of protecting film on the surface.

Acknowledgment

One of the authors, Chandrabhan Verma, gratefully acknowledges North-West University (Mafikeng Campus) South Africa for providing financial supports under postdoctoral scheme.

References

[1] Verma C, Quraishi MA, Olasunkanmi LO, Ebenso EE. RSC Adv. 2015;5:85417–30.
[2] Hejazi S, Mohajernia S, Moayed MH, Davoodi A, Rahimizadeh M, Momeni M, Eslami A, Shiri A, Kosari A. J. Ind. Eng. Chem. 2015;25:112–21.
[3] Haque J, Verma C, Vandana Srivastava MA, Quraishia Eno E, Ebenso,. Res. Phys. 2018;9:1481–93.
[4] Farag AA, Ali TA. J. Ind. Eng. Chem. 2015;21:627–34.
[5] Verma C, Ebenso EE, Bahadur I, Obot IB, Quraishi MA. J. Mol. Liq. 2015;212:209–18.
[6] Hasanov R, Bilge S, Bilgiç S, Gece G, Kılıç Z. Corros. Sci. 2010;52:984–90.
[7] Hasan Basim O, Sadek Sara A. J. Ind. Eng. Chem. 2014;20:297–303.
[8] Dormer PG, Eng KK, Farr RN, Humphrey GR, McWilliams JC, Reider PJ, Sager JW, Volante RP. J. Org. Chem. 2003;68:467–77.
[9] Ayoob AI. Baghdad Sci. J. 2013;10:758–66.
[10] Li Z, Yu M, Zhang L, Yu M, Liu J, Wei L, Zhang H. Chem. Commun. 2010;46:7169–71.
[11] Kalaiselvi K, Nijarubini V, Mallika Rasayan J. J. Chem. 2013;6:52–64.
[12] Manzo RÁ, Canales JM, Cervantes SC, Cruz JM. J. Mex. Chem. Soc. 2013;57:30–5.
[13] Ansari KR, Quraishi MA. Physica E. 2015;69:322–31.
[14] Lebrini M, Robert F, Vezin H, Roos C. Corros. Sci. 2010;52:3367–76.
[15] Nam ND, Somers A, Mathesh M, Seter M, Hinton B, Forsyth M, Tan MYJ. Corros. Sci. 2014;80:128–38.
[16] Fiori-Bimbi MV, Alvarez PE, Vaca H, Gervasi CA. Corros. Sci. 2015;92:192–9.
[17] Yurt A, Duran B, Dal H. Arab. J. Chem. 2014;7:732–40.
[18] Aghzzaf AA, Rhouta B, Rocca E, Khalil A, Caillet C, Hakkou R. Mater. Chem. Phys. 2014;148:335–42.
[19] Goulart CM, Esteves-Souza A, Martinez-Huitle CA, Rodrigues CJF, Maciel MAM, Echevarria A. Corros. Sci. 2013;67:281–91.
[20] Guo L, Ren X, Zhou Y, Xu S, Gong Y, Zhang S. Arab. J. Chem. 2015. https://doi.org/10.1016/j.arabjc.2015.01.005.
[21] Saha SK, Dutta A, Ghosh P, Sukulc D, Banerjee P. Phys. Chem. Chem. Phys. 2015;17:5679–90.
[22] Mukhopadhyaya C, Dasa P, Butcherb RJ. Org. Lett. 2011;13:4664–7.
[23] Mishra A, Verma C, Lgaz H, Srivastava V, Quraishi MA, Ebenso EE. J. Mol. Liq. 2018;251:317–32.
[24] (a) Verma C, Olasunkanmi LO, Quadri TW, Sherif El-Sayed M, Ebenso EE. J. Phys. Chem. C 1882;122(2018):11870–1;
(b) Verma C, Olasunkanmi LO, Ebenso EE, Quraishi MA, Obot IB. J. Phys. Chem. C 2016;120:11598–611.
[25] Yadav DK, Quraishi MA. Ind. Eng. Chem. Res. 2012;51:8194–210.
[26] Li X, Deng S, Xie X. Corros. Sci. 2014;81:162–75.
[27] Roy P, Karfa P, Adhikari UL, Sukul D. Corros. Sci. 2014;88:246–53.
[28] Singh AK, Singh P. J. Ind. Eng. Chem. 2015;21:552–60.
[29] Hussin MH, Kassim MJ. Mater. Chem. Phys. 2011;125:461–8.
[30] Mehdipour M, Ramezanzadeh B, Arman SY. J. Ind. Eng. Chem. 2015;21:318–27.
[31] Barmatov E, Hughes T, Nagl M. Corros. Sci. 2014;81:162–75.
[32] Verma C, Haque J, Ebenso EE, Quraishi MA. Res. Phys. 2018;9:100–12.
[33] Singh AK, Quraishi MA. Corros. Sci. 2010;52:1373–85.
[34] Verma CB, Quraishi MA, Ebenso EE. Int. J. Electrochem. Sci. 2013;8:12894–906.
[35] Ma H, Cheng X, Li G, Chen S, Quan Z, Zhao S, Niu L. Corros. Sci. 2000;42:1669–83.
[36] Singh AK, Quraishi MA. Corros. Sci. 2011;53:1288–97.
[37] Faustin M, Maciuk A, Salvin P, Roos C, Lebrini M. Corros. Sci. 2015;92:287–300.
[38] El-Lateef HMA. Corros. Sci. 2015;92:104–17.
[39] Liu JC, Park SW, Nagao S, Nogi M, Koga H, Ma JS, Zhang GG, Suganuma K. Corros. Sci. 2015;92:263–71.
[40] Behpour M, Ghoreishi SM, Soltani N, Salavati-Niasari M. Corros. Sci. 2009;51:1073–82.
[41] Bammou L, Belkhaouda M, Salghi R, Benali O, Zarrouk A, Al-Deyab SS, Warad I, Zarrok H, Hammouti B. Int. J. Electrochem. Sci. 2014;9:1506–21.
[42] Reddy MJ, Verma CB, Ebenso EE, Singh K, Quraishi MA. Int. J. Electrochem. Sci. 2014;9:4884–99.
[43] Yadav DK, Quraishi MA. Ind. Eng. Chem. Res. 2012;51:14966–79.
[44] Souza FS, Spinelli A. Corros. Sci. 2009;51:642–9.
[45] Verma C, Quraishi MA, Singh A. J. Taiwan Inst. Chem. Eng. 2015;49:229–39.
[46] Yıldız R, Dogan T, Dehri I. Corros. Sci. 2014;85:215–21.
[47] Verma C, Singh P, Quraishi MA. J. Assoc. Arab. Uni. Basic. Appl. Sci. 2016;21:24–30.
[48] Ahamad I, Prasad R, Quraishi MA. Corros. Sci. 2010;52:1472–81.
[49] Yadav DK, Maiti B, Quraishi MA. Corros. Sci. 2010;52:3586–98.
[50] Yana Y, Li W, L. Caia, Hou B. Electrochim. Acta 2008;53:5953–60.
[51] Lvarez PMÁ, García-Araya JF, Beltran FJ, Masa FJ, Medina F. J. Colloid Interface Sci. 2005;283:503–12.
[52] Verma C, Singha P, Bahadur I, Ebenso EE, Quraishi MA. J. Mol. Liq. 2015;209:767–78.
[53] Verma C, Singh A, Pallikonda G, Chakravarty M, Quraishi MA, Bahadur I, Ebenso EE. J. Mol. Liq. 2015;209:306–19.
[54] Verma C, Singh A, Quraishi MA. J. Taiwan. Inst. Chem. Eng. 2015;49:229–39.